

WIND ASSESSMENT IN URBAN AREA WITH CFD TOOLS APPLICATION TO NATURAL VENTILATION POTENTIAL AND OUTDOOR PEDESTRIAN COMFORT

Stéphane Sanquer¹, Guillaume Caniot¹, Sachin Bandhare¹

¹Meteodyn, Nantes, France

ABSTRACT

The paper presents a numerical methodology to assess wind pedestrian comfort and natural ventilation in urban areas. UrbaWind, an automatic computational fluid dynamics code, is improved to model the wind in dense urban environments. The turbulence modelling, that is to say the dependence of turbulence length on the distance from wall, and the model constants are calibrated in order to reproduce precisely flow separation around buildings walls. Numerical results match well with the experiments: separation patterns, pressure field on walls, and wind speed in dense urban area. Two examples are presented at the end of the paper in order to demonstrate the advantages of the methodology for urban designers.

INTRODUCTION

Background

From an urban designer point of view, the knowledge of the urban climatology and especially the wind flow around buildings is crucial in many applications such as:

- Air quality and thermal behavior inside buildings, since air and heat exchange depends on wind pressure on facades. Natural ventilation is the method to reduce energy consumption. This is all the more true since concerns are growing on global warming (Sanquer S., Abdesselam M., Picgirard F., BS 2011)
- Wind energy production from small wind turbines
- Wind comfort in outdoor spaces and in open indoor spaces exposed to wind

CFD tools dedicated to calculating wind flow inside built environment facilitates the understanding and interpretation of the wind in any urban area. Wind mappings become useful to urban designers to optimize the master plan: position and orientation of buildings to improve natural ventilation, small energy production and pedestrians wind comfort (Janssen et al. 2013, Fadl and Karadelis 2013, Szűcz 2013).

In the initial sketch designers should give a technical answer in order to improve the master plan as quickly as possible. As CFD simulations are carried out with a high level of accuracy, this may be time consuming for large and complex urban master plans.

A 1x1 km² urban simulation represents more than 10 million cells. With a standard computer dedicated to consulting services, this implies a computation time exceeding one day for each wind direction.. A short time response is expected during the sketch process whereas computational time can be very long. In that context, a proper methodology needs to be defined to increase the efficiency of the numerical approaches.

Three axes of improvement were highlighted:

- Computation time reduction by improving the meshing process and the solver, using a turbulence model that speeds up the convergence
- For natural ventilation assessment, a macroscopic approach remains the best way to reduce the computational time to obtain the Air Change Rate (ACH). Simulate the flow through windows and inside any buildings in an urban area is not common for consulting services
- Information delivered by CFD tools is not always understandable by designers and may not be used without statistical treatment including the local climatology.

The natural ventilation of a building is driven by the combined forces of wind and thermal buoyancy. However, when openings are large enough and the air change rate is high enough, the indoor temperature is quite homogeneous and, except for important volumes, the natural ventilation is mainly driven by the wind forces. Thus, for the natural ventilation assessment in tropical warm climates, the thermal forces are generally assumed as negligible compared to the wind driven forces. The assessment of the cross-ventilation efficiency is done by considering the wind speed levels inside the buildings, and the flow-rates through the openings or generally the air change rate of the volume (ACH).

The cross-wind flow rate depends on the size of the openings, on their aerodynamic efficiency, namely their aerodynamic discharge coefficients, on the pressure coefficients on the building envelope and on the reference wind velocity upstream the building. Aynsley *et al.* (1977) gave an analytic expression useful for a single ventilated volume with two openings, but as soon as the number of openings is higher or when the internal volume is divided into sub volumes, a resolution for non-linear system has to be used.

All of these characteristics are fundamental and depend on the external wind pressure at the openings. The pressure on the building envelope can be defined with tables (Liddament 1986, Clarke, J *et al.* 1990, Eurocode) or using parametric models based on the analysis of results from wind tunnel tests (Grosso 1992, Muehleisen and Patrizi 2013, Castola *et al.* 2009). These tables or correlations are potentially inapplicable when buildings are irregular and different from the simple shape or when they are surrounded by other buildings in a complex urban area with canyons and corners. In these configurations, the wind strongly fluctuates and the pressure coefficients and wind driven airflows evaluation is subjected to various problems detailed hereafter.

Unfortunately for designers, the pressure value on outside walls of buildings cannot be assessed in urban places with this method for two reasons. The pressure coefficients are highly dependent on the buildings shape and on the influence of neighboring buildings. Moreover, the reference wind velocity needed to convert the pressure coefficient to pressure should not be taken near the project but far enough and high enough above the urban canopy to avoid the inhomogeneity of wind in urban areas. These external wind pressures should be evaluated either from wind tunnel tests (Kandola, 1990) or from computational fluid dynamics (CFD) simulations (Ayad 1999, Fahssis *et al.* 2010, Montazeri and Blocken, 2013).

Analytic methods such as the Aynsley method cannot be used for complex indoor layout where pressure loss occurs. Network aerodynamic tools including pressure loss depending on the internal porosity are necessary to assess the air change rate in such a layout. UrbaWind, a combined CFD-Network software dedicated to modelling the urban climatology, provides the mass flow rate from the computed pressure outdoor field to assess the cross ventilation efficiency (Sanquer *et al.*, 2011). It was shown that ACH depends both on external wall porosity and indoor porosity. The natural ventilation potential can be reduced by 30% with indoor porosity. Nevertheless, without considering the indoor layout the pressure field in a complex urban

area can be analyzed in order to extract natural ventilation potential.

The aim of this work is to present a methodology that allows the quick assessment of urban master plans without carrying out long complex computations, for instance by delivering:

- The natural ventilation potential based on pressure coefficients mappings
- The human comfort index based on wind speeds exceedance statistics

Some validation cases will be presented based on reference round robin tests. Two real examples for various wind exposures and climates illustrate the practical advantages of the approach

NUMERICAL APPROACH: METHODOLOGY AND VALIDATION

Wind computation in any complex urban area

The CFD method of UrbaWind consists of solving the Reynolds-Averaged Navier-Stokes equations on an unstructured rectangular grid with automatic refinement of the mesh near obstacles. The CFD tool delivers the tri-dimensional mean velocity field, the turbulence energy field and the mean pressure for each point in the domain.

$$\frac{\partial \overline{\rho u_i}}{\partial x_i} = 0$$

$$-\frac{\partial (\overline{\rho u_j \overline{u_i}})}{\partial x_j} - \frac{\partial \overline{P}}{\partial x_i} + \frac{\partial}{\partial x_j} \left[\mu \left(\frac{\partial \overline{u_i}}{\partial x_j} + \frac{\partial \overline{u_j}}{\partial x_i} \right) - \overline{\rho u'_i u'_j} \right] + F_i = 0$$

When the airflow is steady and the fluid incompressible, the mean equations for the mean velocity components $\overline{u_i}$ contain unknown quantities. In order to close the system, a one-equation or two-equation model is usually assumed to solve the turbulent fluxes.

The equations resolution is based on a finite volume method with a rectangular multi-bloc refined mesh. A very efficient coupled multi-grid solver is used for a fast convergence for every kind of geometry. (Ferry, 2002). Boundary conditions are automatically generated. The mean velocity profile at the computational domain inlet is determined by the logarithmic law in the surface layer, and by the Ekman function above (Garratt, 1992). A 'Blasius'-type ground law is implemented to model frictions (velocity components and turbulent kinetic energy) at the surfaces (ground and buildings). The effect of porous obstacles is modelled by introducing a volume drag force in the cells lying inside the obstacle.

The transport equation for the turbulent kinetic energy k contains a dissipation term ϵ deduced from the mixing-length theory.

$$\frac{\partial}{\partial x_i} \left[\rho \bar{u}_i k - \left(\frac{\mu_T}{\sigma_k} \right) \frac{\partial k}{\partial x_i} \right] = P_k - \epsilon \quad (1)$$

$$= \mu_T \left(\frac{\partial \bar{u}_i}{\partial x_j} + \frac{\partial \bar{u}_j}{\partial x_i} \right) \frac{\partial \bar{u}_j}{\partial x_j} - \epsilon$$

The turbulence viscosity μ_t is considered as the product of a length scale with a speed scale, which are both characteristic scales of the turbulent fluctuations.

$$\mu_t = \rho k^{1/2} L_T \quad (2)$$

$$\text{and } \epsilon = C_\mu \frac{k^{3/2}}{L_T} \quad (3)$$

The turbulent length scale L_T varies linearly with the distance to the nearest wall d . The dependence of L_T on the distance via a coefficient C_L was defined in order to well reproduce the flow separation around typical building façades and roofs. C_μ is usually fixed at 0.09 for grid turbulence (standard k- ϵ model). In the boundary layer, the C_μ constant depends on the atmospheric stability. The model defining the turbulence length scale by Yamada and Arritt (Hurley, 1997) suggests a dependence of C_μ on the stability criteria in the range of 0.01-0.09. Comparisons with experimental results were made in order to calibrate the C_L and C_μ values for such urban flows.

X_R is the length of the recirculation area in the wake of a tall building sized as 20x20x40 m (figure 1). Velocity magnitude on the wake axis was plot versus the distance from the backward wall (figure 2). Flow separation above the building roof is also highlighted (figure 3) and the flow separation length X_{R_TOP} extracted. All the results were summarized in the table 1. These results were compared with many numerical simulations and experiments of Meng and Hibi (1996) described by Tominaga *et al.*(2008).

The best choice to reproduce both the flow separation in the wake and the upper vortices give a couple of reference values for C_L and C_μ .

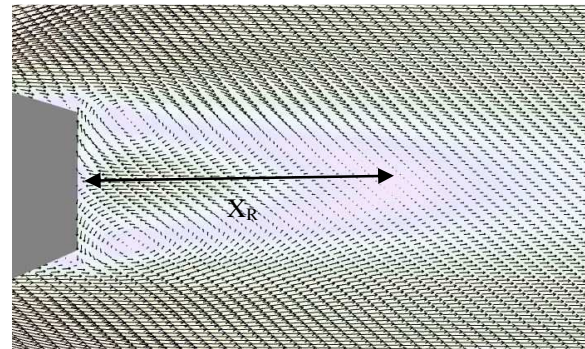


Figure 1 Recirculation in the wake of a square high-rise building

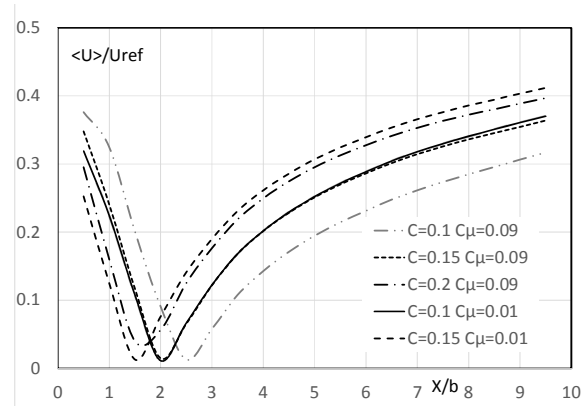


Figure 2 Recirculation in the wake of a square high-rise building

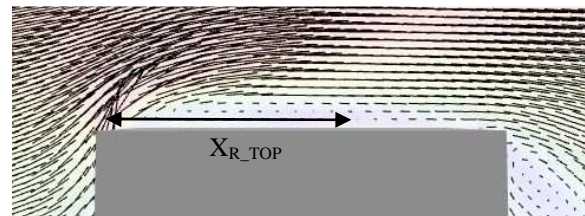


Figure 3 Flow separation above the roof of a square high-rise building

Table 1

Comparison of Numerical models Reattachment length and Experimental values (b is the edge)

Turbulence model	Reference	X_R/b	X_{R_TOP}/b
k- ϵ (Standard)	Tominaga et al.	2.7	No separation
k- ϵ (Modified)	Tominaga et al.	3 to 3.2	0.52 to 0.58
Differential stress model	Mochida et al.	4.2	>1
LES	Tominaga et al.	1 to 2.1	0.50 to 0.62
k-1 ($C_L=0.2, C_\mu=0.09$)	UrbaWind	1.7	0.25
k-1 ($C_L=0.15, C_\mu=0.09$)	UrbaWind	2.5	0.60
k-1 ($C_L=0.1, C_\mu=0.09$)	UrbaWind	2.5	0.70
k-1 ($C_L=0.15, C_\mu=0.01$)	UrbaWind	1.5	0.60
k-1 ($C_L=0.1, C_\mu=0.01$)	UrbaWind	2	0.70
Experiment	Meng and Hibi	1.42	0.52

Air change rate assessment

For a simple volume with two openings, the cross wind flow rate was written by Aynsley et al. (1977):

$$Q = \frac{Cp_1 - Cp_2}{\sqrt{\frac{1}{A_1^2 C_1^2} + \frac{1}{A_2^2 C_2^2}}} U_{WIND} = A_a \sqrt{\Delta Cp} U_{WIND} \quad (4)$$

Where A1 and A2 are the areas of the openings 1 and 2, Cd1 and Cd2 their discharge coefficients given as functions of the openings aerodynamic characteristics, and U_{WIND} is the reference wind velocity.

Hence, mass flow rate depends on three variables: the wind velocity far upstream the buildings U_{WIND}, the aerodynamic area A_a and the pressure differential.

When more than two openings are connected with an indoor volume, the ACH computation needs to use an iterative process: the internal pressure is unknown and the flow rate through openings is solved with a Newton-Raphson iterative method (Fhassis et al. 2010). In the case of a flat with several rooms, the free aerodynamic area of the opening k is replaced by an equivalent aerodynamic surface, taking into account the door aerodynamic surface A_{door} of the secondary room (Sanquer et al., 2011).

$$A_k^{eq} = 1 / \sqrt{\frac{1}{A_k^2} + \frac{1}{A_{door}^2}} \quad (5)$$

All the macroscopic methods use external pressure fields on the walls where the openings are fitted as an input.

Before using a CFD tool to provide pressure values, comparisons were made with experimental data on Silsoe cube (Richards et al., 2007) resumed by Costola et al. (2009). This is a valuable round robin test to check the ability of CFD to capture the flow separation around a cube. The pressure field obtained along the trajectory 0-1-2-3 with UrbaWind matches well the experimental results obtained for a detached low-rise building (figure 4).

Further computations were carried out for the same low-rise building located in a more complex urban environment (figure 6). Various wind incidences were computed; figure 6 shows that the natural ventilation potential defined as the maximum differential of pressure coefficient vanishes in complex urban area. For example ΔCp vanishes from unity (detached, 0°) to less than 0.1 (urban, 0°). For oblique wind incidence (45°), ΔCp vanishes from 0.7 to less than 0.2. This analysis shows the difficulties to extract numerical tables or analytic relations to describe the influence of urban environment since the

signature is the wind aerodynamic interactions with every neighbor buildings.

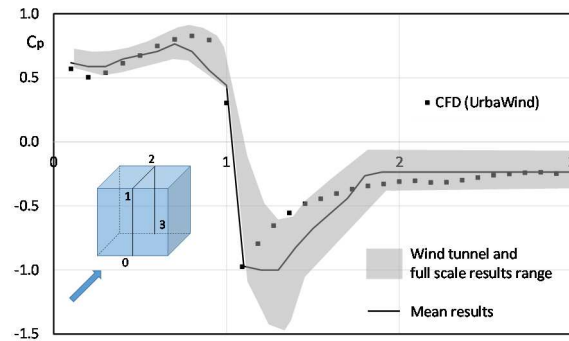


Figure 4 Pressure on the walls of a low-rise detached building: comparison of different wind tunnel experiments and numerical results (UrbaWind)

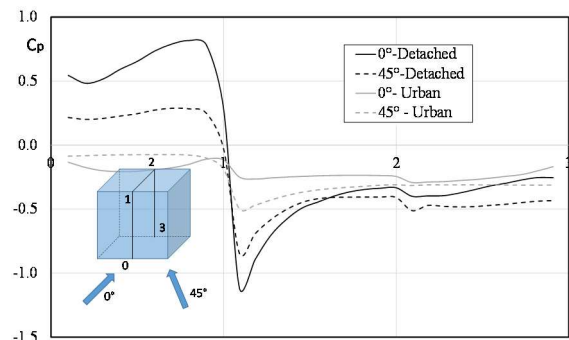


Figure 5 Pressure on the walls of a low-rise building Influence of the urban environment

Complex Urban Wind field and wind comfort analysis

The computed speed-up factors have been compared to the speed-up factors obtained from the experimental measurements. The speed up factor is normalized by a reference wind at 15.9 m height. According to Yoshie et al.(2008) mean scalar velocity measured in the wind tunnel using a non-directive thermistor anemometer is regarded as the time averaged instantaneous scalar velocity whereas the mean scalar velocity given from CFD is calculated from the time averaged velocity vector. Experimental values have been corrected to take into account turbulent kinetic energy.

In figure 7, the computed values generally agree with experimental values (all points). The mean error is equal to 0.04 and the standard deviation error is equal to 0.14.

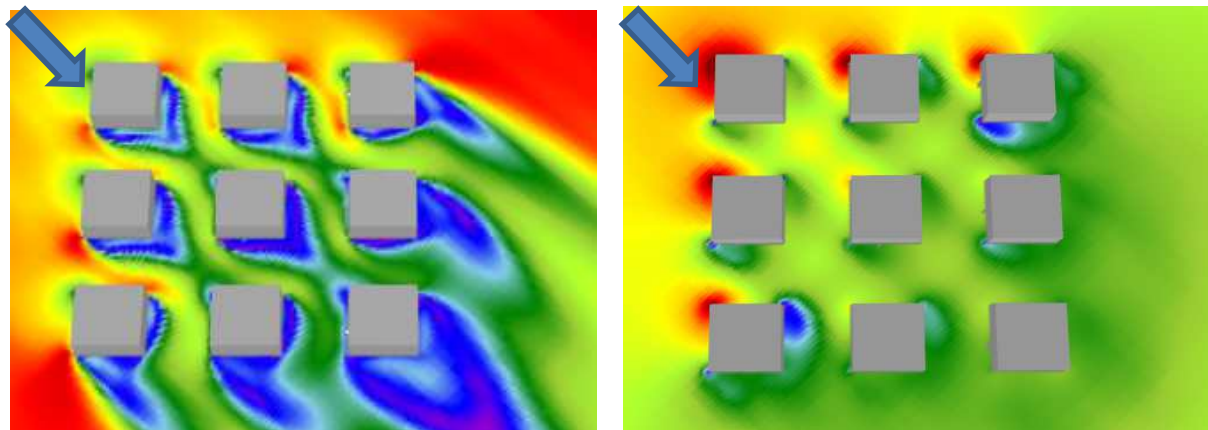


Figure 6 Example of CFD computation in complex urban area: wind speed (left) and pressure (right)

The 77 probes, located at 2 meters height in the full-scale experiment, are represented in red in figure 8. When error ($|C_{Exp} - C_{CFD}|$) is above 0.1, 38 experimental values are displayed in figure 8 and by red points in figure 7.

The distribution of those points with an error above 0.1 tends to be quite homogeneous in the flow pattern.

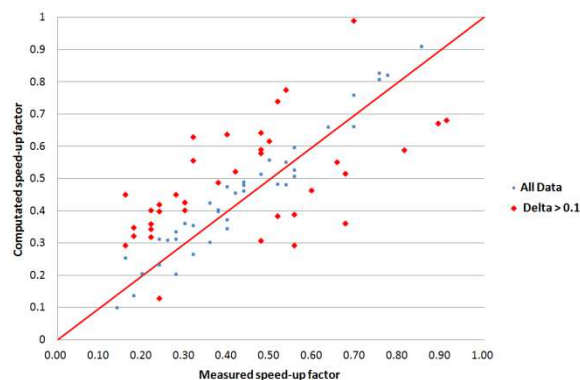


Figure 7 Measurement Vs Computed Speed Up Factor (red points correspond to error > 0.1)

As noted by Yoshie et al.(2008), CFD results often tend to underestimate the wind speed in the wake region of the building. The difference between the scalar velocities in the wake region from the CFD and the experimental results is partly because the definition of the mean scalar velocity measured by the non-directivity thermistor anemometers was different from that of CFD.

Once several directional computations are computed, one can assess mean wind speed and turbulence intensity thanks to mast weather data.

The wind comfort is expressed in terms of rates of wind speed thresholds exceedance as recommended by Delpech et al. (2005). If we apply for instance the CSTB criteria, we consider the frequency of the “gust speed” exceeds 3.6 m/s. In this case, the “gust speed” is defined as the sum of the 10 min mean wind speed and its standard deviation.

According to CSTB criteria, the limit of comfort is 5% exceedance for a steady position, 10% for a walking pedestrian, and 20% for a brisk walking.

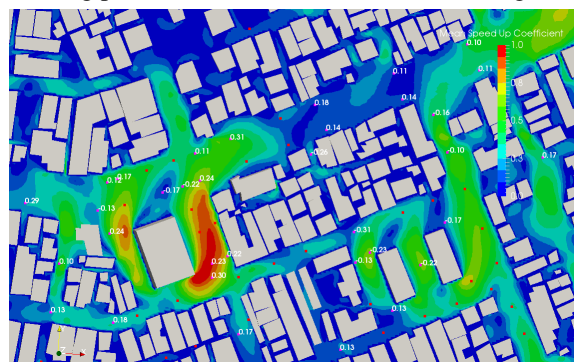


Figure 8 Computed Wind Speed Coefficient map in red and difference between computed and experimental data

Table 2
Discomfort frequency

	Transitory motion	Recreational motion	Short Stationary	Long Stationary
France	$F(V > 3.6) < 20\%$	$F(V > 3.6) < 10\%$	$F(V > 3.6) < 5\%$	$F(V > 3.6) < 5\%$
Netherlands	$F(V > 5) < 20\%$	$F(V > 5) < 10\%$	$F(V > 5) < 5\%$	$F(V > 5) < 5\%$
Denmark	$F(V > 5) < 50\%$	$F(V > 5) < 34\%$	$F(V > 5) < 15\%$	$F(V > 5) < 15\%$
Montreal (Winter)	$F(V > 4) < 25\%$	$F(V > 4) < 15\%$	$F(V > 4) < 10\%$	$F(V > 4) < 10\%$
Montreal (Summer)	$F(V > 6) < 25\%$	$F(V > 6) < 15\%$	$F(V > 6) < 10\%$	$F(V > 6) < 10\%$
United Kingdom	$F(V > 11) < 2\%$	$F(V > 8) < 4\%$	$F(V > 5) < 6\%$	$F(V > 5) < 1\%$

Notation: $F(V > 3.6)$ = frequency of the winds faster than 3.6 m/s

EXAMPLES OF APPLICATIONS

Natural ventilation potential in tropical humid warm climate

The first example is located at the Reunion Island where trade winds are moderate on the north side of the island. Even in urban areas the average velocity is close to 2 m/s at 10 m above the ground and the buildings may be naturally ventilated. Moreau and Gandermer (2002) gave some recommendations to assess the potential of natural ventilation in tropical warm climates. Guidelines are based on the pressure coefficient differential ΔC_p between upwind and downwind side walls of a building (table 3).

Table 3
Guidelines for Natural ventilation potential

Level of natural ventilation efficiency	ΔC_p range
ACH too low	$\Delta C_p < 0.17$
ACH enough	$0.17 \leq \Delta C_p < 0.39$
ACH good	$0.39 \leq \Delta C_p < 0.53$
ACH very good	$0.53 \leq \Delta C_p$

Some mappings of ΔC_p are shown for a part of the urban district for the main wind direction. Colored arrows were over printed on buildings in order to optimize the openings characteristics. The buildings layout may be optimized in order to allow enough pressure on walls for each volume. Some of them, due to the orientation of the façades and the wind shield of the others buildings, could not be naturally ventilated. In these cases, mechanical ventilation could be chosen for some specific rooms.

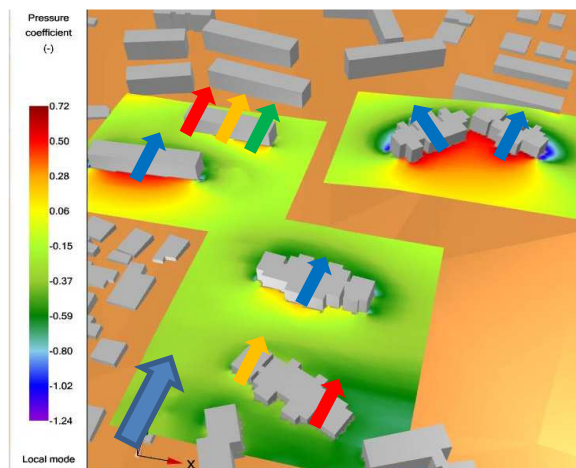


Figure 9 Pressure field mapping to assess the potential of natural ventilation (La Réunion Island)

Porosity of façades was defined according to the variability of ACH and of thermal loads that depend

on the location of the volume in the building (ground, middle, top) and on the location of the building in the master plan (exposed, protected, shaded by nearby buildings). Thermal design was carried out according to the simple methodology Batipei commonly used in such tropical overseas territories and presented in a previous BS conference (Sanquer *et al.* 2011)

A second example concerns a project in French Guiana. Close to the equator Trade winds are weaker and the average wind speed is below 2 m/s at 10 meters above the ground. In this situation, colored arrows were also printed in order to highlight the potential to help the urban design according to the table 3 criteria. Urban designers used this diagnostic mapping to change the layout and to find a compromise that avoids the case of under ventilation of volumes. The strategy consists of increasing the pressure coefficient differential above the limit of 0.2 for all the ventilated spaces as much as possible.

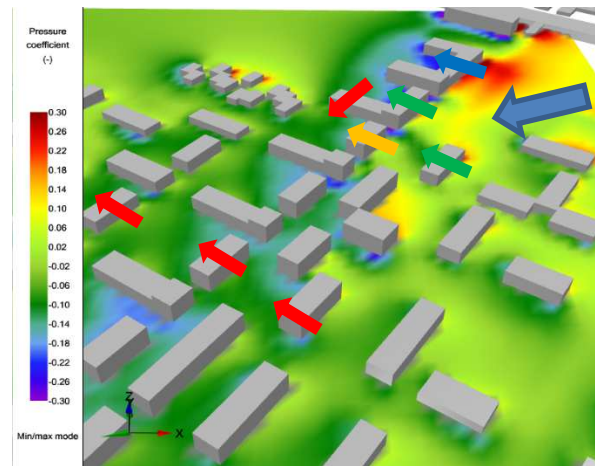


Figure 10 Pressure field mapping to assess the potential of natural ventilation (French Guiana)

Wind comfort in a reshaping area in Paris

This example is located in Paris on Seguin Island. The reshaping of 0.12 km² area includes 29 400 m² of terrace and 12 000 m² of park. The wind comfort assessment is critical in those pedestrian areas (overall on the rim of the island) where the closest building on the opposite river bank is located from 60 m to 100 m to Seguin Island.

The prevailing winds are coming from the South to West-South-West (240 deg) representing 30 % of the wind frequency.

Several wind acceleration effects responsible for wind discomfort can be seen on figure 11 below:

- Corner Effect on 1
- Venturi Effect on 2 and 3

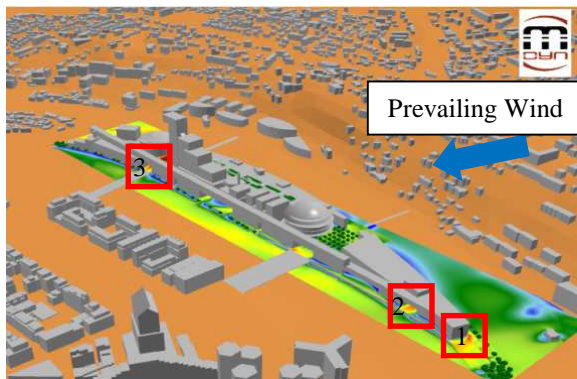


Figure 11 Pedestrian Wind comfort assessment on Seguin Island in Paris

Only the East side of the Island is suitable for long or short stationary positions.

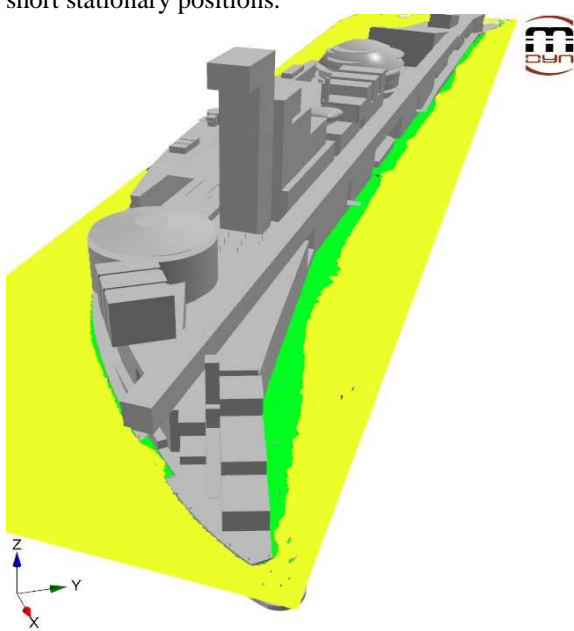


Figure 12 Pedestrian Wind comfort (green area is suitable for stationary position whereas yellow is not comfortable for this activity)

Local treatments such as vegetation or fences can prevent such strong acceleration and enhance the wind comfort.

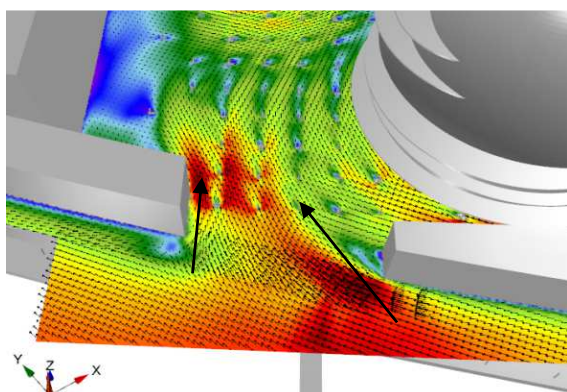


Figure 13 Corner effect causing strong acceleration (red color) can be reduced with windbreaks

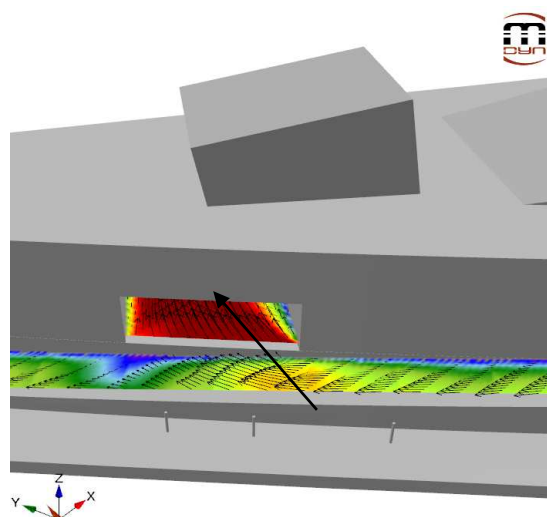


Figure 14 Venturi effect causing strong acceleration (red color) can be reduced with windbreaks

CONCLUSION

The paper presents a numerical methodology to assess the wind pedestrian comfort and the natural ventilation in any urban area.

UrbaWind, an automatic computational fluid dynamics code, was developed to model the wind in urban environments by optimizing the meshing and solving processes. Accurate results computed as quickly as possible will be useful for urban designers.

The turbulence modelling, namely the dependence of turbulence length on the distance from wall and the C_{μ} value of the k-l model were calibrated in order to well reproduce the flow separation around buildings walls. Numerical results were compared with well documented experiments: Siloe cube as a low-rise building and a 1:1:2 tower as high-rise buildings and Nigata urban case. Comparisons were made on separation patterns, pressure fields on walls and wind speed on pedestrian path walks. Some real examples are presented at the end of the paper in order to demonstrate the advantages of the methodology for urban designers.

REFERENCES

- Sanquer S., Abdesselam M., Picgirard F., 2011, Combined CFD-mean energy balance method to thermal comfort assessment of buildings in a warm tropical climate, Building Simulation
- Janssen W., Blocken B., Hooff T.V., 2013, Use of CFD simulations to improve the pedestrian wind comfort around a high-rise building in a complex urban area, 13th conference of international building performance simulation association, Chambéry, France, pp 1918-1925

- Fadl M.S., Karadelis J., 2013, CFD simulation for wind comfort and safety in urban area: a case study of Coventry university central campus, *International Journal of Architecture, Engineering and construction*, Vol.2, No.2, pp 131-143
- Szücs A., 2013, Wind comfort in a public urban space – case study within Dublin Docklands, *Frontiers of architectural Research*, 2, pp 50-66
- Aynsley R.M, Melbourne. W., Vickery B.J., 1977, *Architectural aerodynamics*, Applied science Publishers London
- Liddament, M. W., 1986, *Air Infiltration Calculation Techniques*, An Applications Guide, AIVC.
- Clarke J, 1990, Hand J, Strachan P, A building and plant energy simulation system. Energy Simulation Research Unit, Department of Mechanical Engineering, University of Strathclyde.
- Eurocode 1: Actions on structure – Part 1-4 : general actions – Wind Actions, EN 1991-1-4, CEN/TC 250
- Grosso M, 1992 Wind pressure distribution around buildings: A Parametrical Model, *Energy and Building*, 18: pp 101-131.
- Muehleisen R.T., Patrizi S., 2013 A new parametric equation for the wind pressure coefficient for low-rise buildings, *Energy and Building*, 57: pp 245-247.
- Costola D., Blocken B., Hensen J.L.M, 2009, Overview of pressure coefficient data in building energy simulation and airflow network programs, *Building and Environment*, 44, pp 2027-2036
- Kandola B.S., 1990, Effects of atmospheric Wind on flows through natural convection roof vents, *Fire technology*, 05-1990, pp106-120
- Ayad S.S., 1999, Computational study of natural ventilation, *Journal of Wind Engineering and Industrial Aerodynamics*, 82, pp 49-68
- Fahssis K., Dupont G., Leyronnas P., 2010. UrbaWind, a Computational Fluid Dynamics tool to predict wind re-source in urban area, *International Conference of Applied Energy*, Conference paper, April 2010, Singapore
- Montazeri, H. Blocken B., 2013, CFD simulation of wind-induced pressure coefficients on buildings with and without balconies: validation and sensitivity analysis, *Building and Environment*, 60, pp 137-149
- Sanquer S., Caniot G., Li W., Delaunay D., 2011, A combined CFD-Network method for the cross-ventilation assessment in buildings, 13th International Conference on Wind Engineering, Amsterdam
- Ferry M., 2002. New features of the MIGAL solver, in: *Proceedings. Phoenix Users International Conference*, Mos-cow, Sept 2002
- Garratt J.R., 1992, *The atmospheric boundary layer*, Cambridge Atmospheric and space sciences series.
- Hurley P.J., 1997. An evaluation of several turbulence schemes for the prediction of mean and turbulent fields in complex terrain
- Meng T., Hibi K., 1998. Turbulent measurements of the flow field around a high-rise buildings. *Journal of Wind Engineering, Jpn*, 76, pp 55-64
- Tominaga, Y., Mochida, A., Murakami S., Sawaki S., 2008. Comparison of various revised k-ε models and LES applied to flow around a high-rise buildings model with 1:1:2 shape placed within the surface boundary layer. *Journal of Wind Engineering and Industrial Aerodynamics*, 96, pp 389-411
- Tominaga, Y., Mochida, A., Yoshie, R., Kataoka, H., Nozu, T., Yoshikawa, M., Shirasawa, T., 2008. AIJ guidelines for practical applications of CFD to pedestrian wind environment around buildings. *Journal of Wind Engineering and Industrial Aerodynamics*, 96, 1749-1761
- Richards P.J., Hoxey R.P., Connel B.D., Lander D.P., 2009, Wind tunnel modelling of the Silsoe cube, *Journal of wind engineering & industrial aerodynamics*, 95, pp 1384-1399
- Yoshie, R., Mochida, A., Tominaga, Y., Kataoka, H., & Yoshikawa, M. (2005). Cross comparisons of CFD prediction for wind environment at pedestrian level around buildings. Part, 1, 2648-2660. *Cross Comparisons of CFD Prediction for Wind Environment at Pedestrian Level around Buildings*
- Delpech P., Baker C.J., Blackmore P.A., Koss H., Sanz-Andres A., Stathopoulos T. Willemsen E., 2005. Pedestrian wind comfort assessment criteria: A comparative case study, *Proc. 4th European & African Conference on Wind Engineering*, 11-15 July 2005, Prague
- Moreau S. and Gandemer J., 2002, *Guide sur la climatisation naturelle de l'habitat en climat tropical humide. Tome III Principes aérodynamiques de la ventilation naturelle dans l'habitat tropical collectif – CSTB – ISBN 2-86891-302-4*
- Sanquer S., Abdesselam M., Picgirard F., 2011, Combined CFD-Mean Energy Balance method to thermal comfort assessment of buildings in a warm tropical climate, *Buildings Simulation Conference 2011*, Sydney